Journal of Crystal Growth 311 (2009) 4486–4490

Contents lists available at ScienceDirect

Journal of Crystal Growth

journal homepage: www.elsevier.com/locate/jcrysgro

Ordered arrays of high-quality single-crystalline α-Si_3N_4 nanowires: Synthesis, properties and applications

Mashkoor Ahmad, Jiong Zhao, Caofeng Pan, Jing Zhu *

Beijing National Center for Electron Microscopy, The state key Laboratory of New Ceramics and Fine Processing, Laboratory of Advanced Material, China Iron & Steel Research Institute Group, Department of Material Science and Engineering, Tsinghua University, Beijing 100084, China

ARTICLE INFO

Article history:
Received 14 January 2009
Received in revised form
25 June 2009
Accepted 9 August 2009
Communicated by J.M. Redwing
Available online 18 August 2009

PACS:
81.07.Bc
81.05.Hd
68.37.Og
61.46.-w

Keywords:
A1. Ordered arrays
A2. Crystalline
B1. α-Si_3N_4 nanowires

ABSTRACT

Ordered arrays of high-quality single-crystalline α-Si_3N_4 nanowires (NWs) have been synthesized via thermal evaporation and detailed characteristics of the NWs have been analyzed by employing scanning electron microscope (SEM) along with energy dispersive spectroscopy (EDS), high-resolution transmission electron microscope (HRTEM), X-ray diffraction (XRD), X-ray photospectroscopy (XPS), infrared (IR), photoluminescence (PL) and in situ I–V measurements by STM/TEM holder. The microscopic results revealed that the NWs having diameter in the range of ~30–100 nm and length in microns. Furthermore, the NWs are found to be single crystalline grown along [0 0 1] direction. The elemental composition and valence states of elements are analyzed by EDS and XPS. The room temperature PL spectra exhibit a broad range visible emission band. The electron transport property of a single NW illustrates the symmetric I–V curve of a semiconductor. The possible growth mechanism is also briefly discussed.

1. Introduction

One-dimensional (1D) nanostructures of nitrides semiconductors have attracted much attention because of their improved performance, compared to the 2D or 3D semiconductor devices. At present research still makes an effort to develop high-quality nitride nanomaterials to obtain high efficiency devices. Among the IV-nitrides, the Si_3N_4 is one of the outstanding functional material and has been applied in various fields due to good performance in mechanical, chemical, electronic and thermal properties [1,2]. It is also a wide band gap (~5.3 eV) semiconductor in which mid-gap levels can be introduced by properly doping, in order to tailor its electronic/optic properties [3,4]. Similar to the group III-N compounds, such as GaN and AlN, Si_3N_4 is also one of the most important technical ceramics owing to its interesting properties, such as high bending strength [5], low density, good resistance to corrosion and oxidation [6,7], excellent chemical stability [8] and so forth. In addition, it is usually two types of structural modification, low temperature-phase trigonal α-Si_3N_4 [9] and stable hexagonal β-Si_3N_4 [10]. These properties favor Si_3N_4 as a suitable material for a wide range of engineering applications.

Recently, among different morphologies ordered arrays of α-Si_3N_4 nanowires (NWs) have great attention due to their novel chemical and physical properties for future applications in nanodevices. To date 1D Si_3N_4 in the shapes of wires, rods and belts has been synthesized by employing different routes. Gundiah et al. [11] synthesized Si_3N_4 NWs through the reaction of silica gel and multi-walled carbon nanotubes at 1350 °C in the presence of Fe catalyst in NH_3. Zhang et al. [12,13] reported the synthesis of Si_3N_4 NWs by Si powders or Si/SiO_2 powder mixture in N_2 or NH_3 atmosphere with or without Fe or Ni powders. Kim et al. [14] synthesized α-Si_3N_4 NWs directly through the reaction of silicon substrate and NH_3, using gallium (Ga), gallium nitride (GaN) and iron (Fe) nanoparticles as catalyst. Wu et al. [15] synthesized Si_3N_4 NWs sheathed with silicon and silicon oxide through the reaction of silicon oxide nanoparticles and active carbon. Han et al. [16] obtained a mixture of α- and β-phase silicon nitride NWs using carbon nanotubes as a template to react with Si/SiO_2 powder mixture in nitrogen atmosphere. Wang et al. [17] reported a sol–gel route for large scale synthesis of Si_3N_4 NWs and nanotubes. Fengmei Gao et al. [18] synthesized aligned Si_3N_4 NWs via pyrolysis of a polyaluminasilazane precursor.

* Corresponding author. Fax: +86 10 62771160.
E-mail address: Jzhu@mail.tsinghua.edu.cn (J. Zhu).

0022-0248/$ - see front matter © 2009 Elsevier B.V. All rights reserved.
doi:10.1016/j.jcrysgro.2009.08.003

In spite of these tremendous efforts, the synthesis of ordered arrays of α-Si_3N_4 NWs and their detailed characteristics have not been still reported. In this work, arrays of NWs have been first synthesized via thermal evaporation and their detail characteristics have been analyzed by employing many techniques. The present study may open up new approaches for the synthesis and the applications of arrays of α-Si_3N_4 NWs.

2. Experimental

Synthesis of ordered arrays of α-Si_3N_4 NWs were carried out in a horizontal quartz tube furnace via thermal evaporation method, where the temperature, pressure and flow rates of working gases are well controlled. A Si with Ni coated as catalyst was used as a substrate. It was cleaned carefully, followed by supersonically in acetone, alcohol and de-ionized water for 10 min. A crucible containing the Ga as source material was placed in the central region of the quartz tube furnace. Si substrate was loaded on the top of the alumina boat and the distance between the substrate and the Ga was about 3 mm. The quartz tube was degassed under vacuum and purged with ammonia. Ammonia was introduced into the quartz tube with a flow rate of 150 sccm. The temperature of the furnace was increased in the range of ~900–1200 °C from room temperature and kept for 3 h under a constant flow of ammonia. A series of experiments were performed with the same conditions except temperature. After the quartz tube was cooled down to room temperature the ammonia flow was turned off. The morphology of the as-prepared products was first examined by scanning electron microscope (SEM-6301F) along with EDS. An ordered arrays of α-Si_3N_4 NWs were obtained at 1100 °C. At this temperature reproducible results were found by repeating the experiments. The detailed characteristics were examined by scanning electron microscope (SEM) along with energy dispersive spectroscopy (EDS), high-resolution transmission electron microscope (HRTEM), X-ray diffraction (XRD), X-ray photospectroscopy (XPS), infrared (IR), photoluminescence (PL) and in situ I–V measurements by STM/TEM holder inside the 200 kV TEM (JOEL-2010F) with a two-terminal configuration.

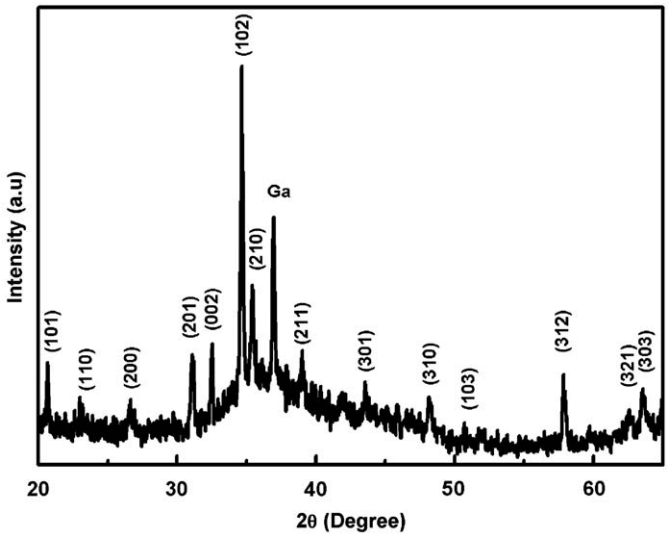

Fig. 1. XRD pattern of the ordered arrays of α-Si_3N_4 NWs.

3. Result and discussion

The structures of the as-grown products have been characterized by X-ray diffraction. Fig. 1 shows the XRD pattern of the ordered arrays of α-Si_3N_4 NWs on Si substrates. It reveals the overall phase composition and purity of the product. All the peaks are in good agreement with α-phase Si_3N_4 NW and at the same position as that of the reported one (JCPDS card no. 41-0360). The

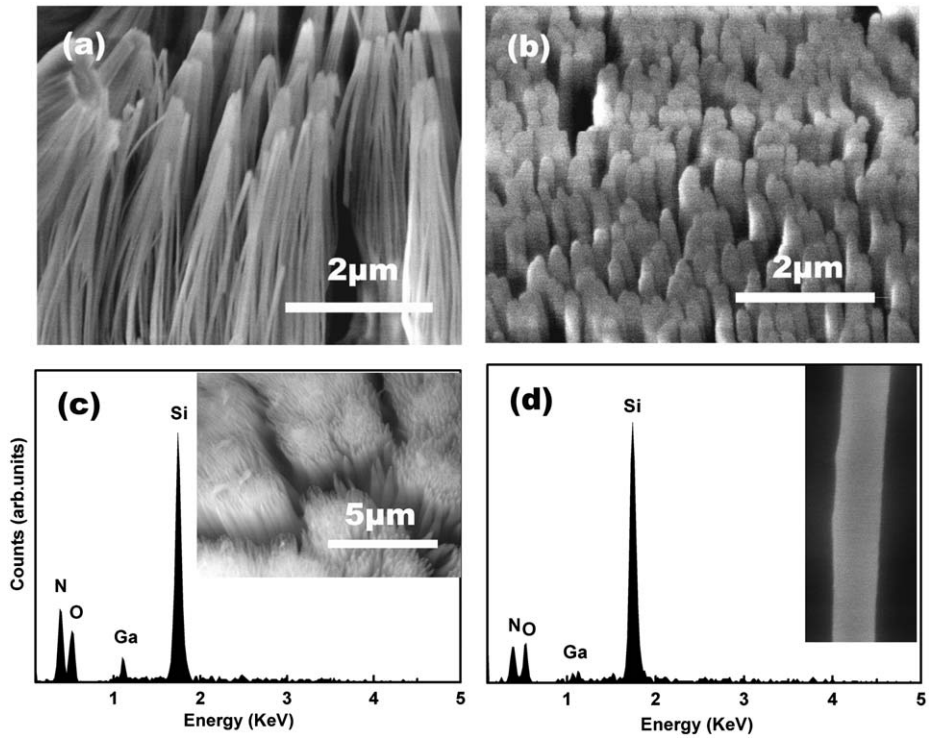

Fig. 2. (a) SEM image of the side view of α-Si_3N_4 NWs, (b) top view, (c) EDS spectra of the NWs in bulk, low magnified SEM image of the NWs (inset), (d) EDS spectra of the single NW, magnified SEM image of the single NW (inset).

Ga peak is also observed in the spectrum which is due to the source material. The lattice constant calculated from the XRD pattern are 7.7428 Å for *a*, and 5.6383 Å for *c*, which are consistent with those of α-Si_3N_4 ($a = 7.7541$ Å, $c = 5.6217$ Å).

Figs. 2(a and b) show the side view and top view SEM morphology of α-Si_3N_4 NWs arrays deposited on the Si substrate after 3 h reaction at 1100 °C. The observation reveals that the product composed of high density ordered arrays of α-Si_3N_4 NWs. These NWs are straight and uniform with diameter in the range of ~30–100 nm and length in microns. Fig. 2(c) shows the low magnified SEM image (inset) and corresponding EDS spectrum while Fig. 2(d) shows the single NW (inset) and their corresponding EDS spectrum. Both spectra demonstrate that the product mainly composed of silicon and nitrogen elements with atomic ratio of about 3:4. Two small weak peaks of O and Ga are also observed due to amorphous layer and source material respectively.

The microstructure of the NWs has been further investigated by using HRTEM. Fig. 3(a) shows the TEM and HRTEM image of individual α-Si_3N_4 NWs. It demonstrates that α-Si_3N_4 NWs have single-crystalline nature with an outer edge amorphous layer and grown in the [0 0 1] direction. The spacing distances between two adjacent fringes in different planes are calculated as shown in Fig. 3(a). These spacing distances are also consistent with the lattice constant of bulk α-Si_3N_4 (JCPDS card no. 41-0360). The corresponding selected area ED (SAED) pattern is identical over the entire NW as shown in Fig. 3(b). The lattice constants calculated from the SAED are 7.7365 Å for *a*, and 5.6133 Å for *c*, which are also consistent with those of α-Si_3N_4 ($a = 7.7541$ Å, $c = 5.6217$ Å).

To distinguish between local and global concentrations, the valence states of elements have been analyzed by XPS. Fig. 4(a and b) shows the XPS spectra of Si2p and N1s level for α-Si_3N_4 NWs.

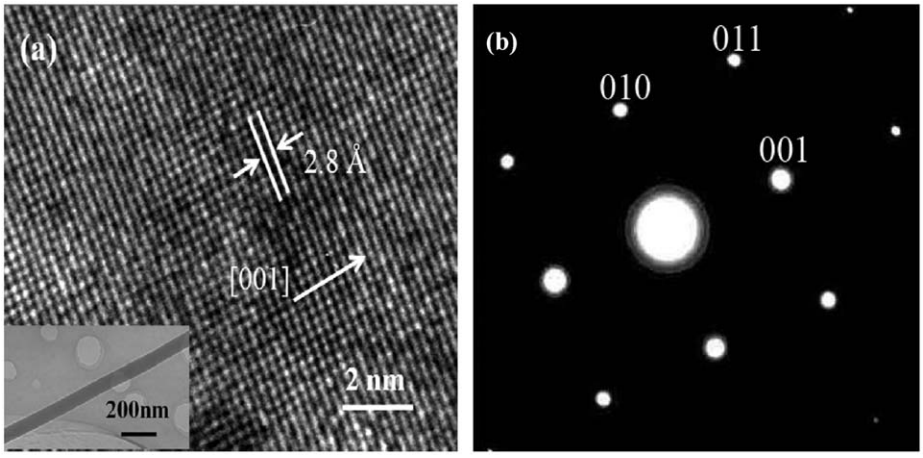

Fig. 3. (a) HRTEM image shows a high-quality crystalline α-Si_3N_4 NWs grown along [0 0 1] direction, corresponding TEM image of single NW (inset), (b) corresponding SAED pattern.

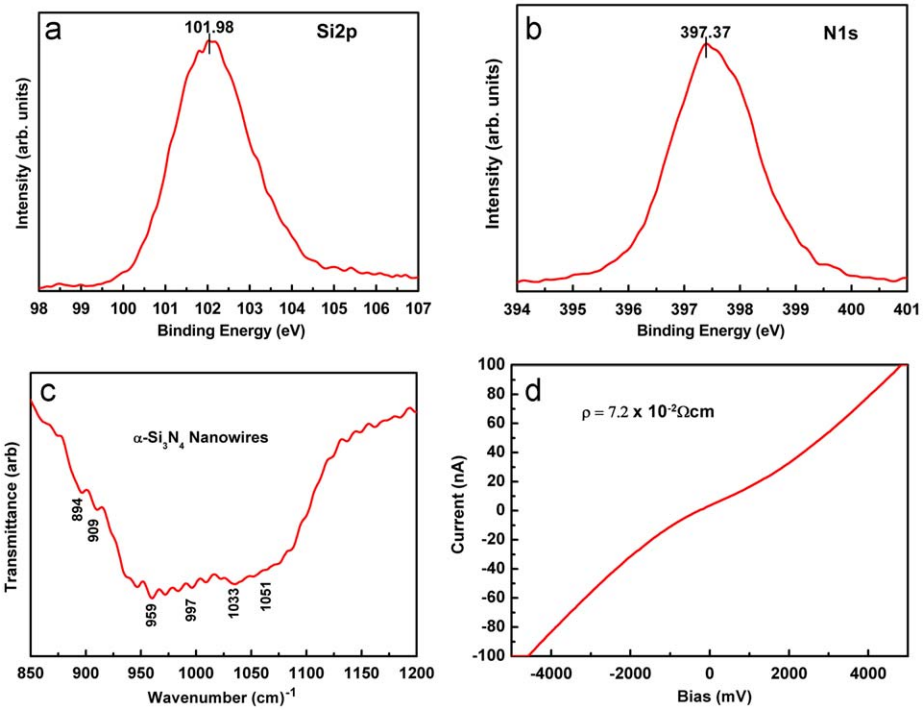

Fig. 4. XPS spectra of the product (a) Si2p and (b) N1s, (c) IR spectrum of the ordered arrays of α-Si_3N_4 NWs, (d) in situ I–V curve of the single α-Si_3N_4 NW illustrates the symmetric behavior.

The XPS gives the NWs surface composition locally while EDS gives the bulk of the product. From XPS analysis the peaks located at 101.98 and 397.37 eV correspond to the electronic states of Si2p, N1s, respectively, which are also in agreement with the data reported [19]. Besides silicon and nitrogen, the spectra also display two other small weak peaks at 532.32 and 284.76 eV, which may come from surface oxidation layer and hydrocarbons. The N atomic concentration ratio measured by XPS is much higher than the one measured by EDS.

The IR spectrum of the product has been shown in Fig. 4(c). It demonstrates a wide absorption band in the range of 900–1200 cm^{-1}, with a maximum peak of 959 cm^{-1}. This band is ascribed to the Si–N stretching vibration mode of α-Si_3N_4 NWs [20]. It is observed that the series of the peaks show a redshift which may be attributed to the nanosize effect as reported [21]. With regard to NWs with smaller diameter, tensile and compressive stress affects the IR spectra line by redshift, and microcrystals smaller than 30 nm lead to downshift and broadening [22]. The IR spectrum also provides good evidence for the synthesis of high-quality α-Si_3N_4 NWs.

The measurements of I–V curves have been carried out by in situ TEM as done by [28], in order to investigate the electrical properties of the arrays of α-Si_3N_4 NWs. Fig. 4(d) shows I–V curve of individual α-Si_3N_4 NW after establishing a contact between W tip-α-Si_3N_4 NW and Au-electrode for the in situ measurement inside TEM, which is clearly illustrating almost symmetric behavior of a semiconductor. This shows that a Schottky contact is formed at each end of α-Si_3N_4 NW and allows the device to function like two reversely connected Schottky diodes as repotted [29]. It has been shown that the Schottky barrier height at the metal–semiconductor interface has a direct effect on the non-linearity of the I–V curve [30]. Multiple I–V curves as well as calibration experiments on more than 20 NWs have been performed to ensure reproducibility. Due to the perfect contacts between α-Si_3N_4 NW and the two electrodes, the I–V curve has excellent repeatability. In a high bias regime where the I–V response is linear, the I–V curve can be differentiated to obtain a resistance R of α-Si_3N_4 NW by using the relation, $R \sim dV/dI$. This is because at high bias the majority of the voltage drop is distributed to the NW itself, whereas at a low bias the majority of the voltage drop is distributed to the Schottky barriers. Thus I–V curve gives the total resistance about $55 \times 10^6\,\Omega$ of the single NW. To calculate other parameters Zhang et al. method [30] has been applied. Using this approach along with the measured diameter and length of the NW, the resistivity of α-Si_3N_4 NW is calculated to be $7.2 \times 10^{-2}\,\Omega\,cm$.

Fig. 5 shows the room temperature PL spectra of the synthesized α-Si3N4 NWs arrays from four different points. The NWs show visible luminescence giving a broad range emission band between 500 and 700 nm with a maximum peak at 610 nm (2.04 eV). The broad visible emission band is divided into four peaks at 416 nm (2.98 eV), 585 nm (2.12 eV), 610 nm (2.03 V) and 686 nm (1.8 eV). Three small UV peaks are also observed at 390, 402 and 416 nm. Previous studies have revealed that PL bands with the peak positions of 2.0–3.2 eV are closely related to the defect energy levels, such as those of Si–Si, N–N, ≡Si and =N [23–26]. The presence of surface oxygen species will inevitably form Si–O–Si and N–Si–O structure defects and introduce corresponding Si–O–Si and N–Si–O defective gap states, which leads to the emissions around 2.5 and 2.8 eV, respectively [27]. In our results, we believe that the physical origin of this broad emission band can be due to the incorporation of Ga during the synthesis of NWs. The presence of Ga–Si–N form defect states and give rise to levels within the gap between conduction and valence band. Therefore, it can be deduced that these defect energy levels are responsible for the broad emission band of the α-Si_3N_4 NWs.

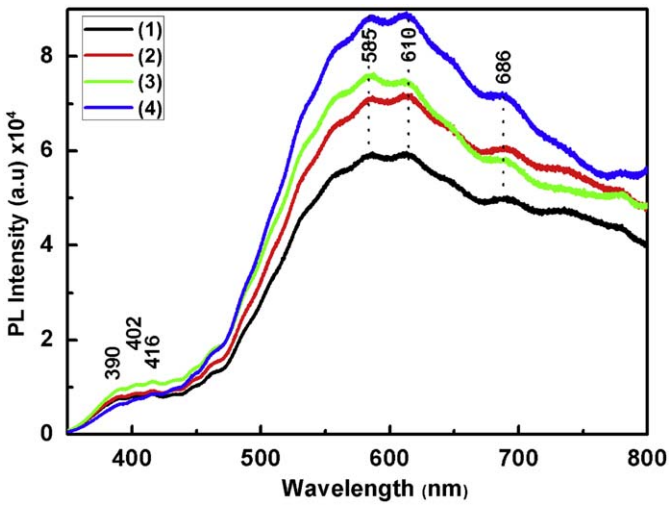

Fig. 5. Room temperature PL spectrum of the ordered arrays of α-Si_3N_4 NWs from four different points.

As we observed from the SEM and TEM images that no droplet of any catalyst has been seen at the top of any NW, vapor–liquid–solid (VLS) mechanism is excluded. The NWs might grow via root growth model. During the growth process of ordered arrays of NWs both the chemical and physical processes are possible. In our previous study, Ga and Ga_2O_3 mixture with Fe catalyst has been used for the synthesis of aligned and non-aligned NWs [31], but in the present work gallium is used as source material with Ni catalyst. We observed Ni thin film increases significantly the yields and may provide a good environment for the synthesis of ordered arrays of α-Si_3N_4 NWs at 1100 °C. On the basis of the above experimental results, a growth model for synthesizing α-Si_3N_4 NWs is suggested. In this model the growth of NWs is divided into two steps. In the first step, at the reaction temperature, nickel will react with silicon and produces nickel silicides that play the role of catalyst in the formation of NWs. In the second step, at high temperature, ammonia will decompose stepwise to NH, NH_2 and N and then directly react with the supersaturated silicon atoms in the nickel silicides to form the nucleation of Si_3N_4 NWs with the following reaction equation.

$$3Si(s) + 4NH_3(g) \overset{Ni(catalyst)}{\longrightarrow} Si_3N_4(s) + 6H_2(g)$$

Once the nucleation forms, the growth of Si_3N_4 NW starts and extends in the axial direction. The unidirectional motion of reactants atoms cloud driven by the carrier gas may also plays an excellent role in the growth of arrays of NWs at a particular temperature.

4. Conclusion

In conclusion, ordered arrays of α-Si_3N_4 NWs have been successfully synthesized via thermal evaporation method. It has been revealed that the NWs have diameter in the range of ~30–100 nm and length in microns. The NWs are found to be single crystalline and grown along [0 0 1] direction via root growth model. Furthermore, the broad visible emission band of NWs may open possibilities for the utilization in optoelectronic devices. In addition, a series of experiments revealed that the Ni catalyst at 1100 °C play a very important role for the synthesis of ordered arrays of α-Si_3N_4 NWs. It has been investigated that the NWs morphology could be precisely tuned via controlling temperature.

The electrical conductance of the NWs makes them potential in the integration of future novel nanodevices and nanocomposites.

Acknowledgments

This work was financially supported by the National 973 Project of China and the Chinese National Natural Science Foundation.

References

[1] Riley, Ceram. Technol. Int. 55 (1993) 8.
[2] J. Lis, S. Majorowski, J. Hlavacek, J. Am. Ceram. Bull. 70 (1991) 244.
[3] F. Munakata, K. Matsuo, K. Furuya, Y.J. Akimune, I. Ishikawa, Appl. Phys. Lett. 74 (1999) 3498.
[4] A.R. Zanatta, L.A.O. Nunes, Appl. Phys. Lett. 72 (1998) 3127.
[5] C.F. Pan, J. Zhu, J. Mater. Chem. 19 (2009) 869.
[6] H. Chen, Y.G. Cao, X.W. Xiang, J.T. Li, C.C. Ge, J. Alloys Compd. 325 (2001) L1.
[7] C.C. Tang, Y. Bando, T. Sato, K. Kurashima, J. Mater. Chem. 12 (2002) 1910.
[8] G. Ziegler, J. Heinrich, C. Wotting, J. Mater.Sci. 22 (1987) 3041.
[9] K. Kato, Z. Inoue, K. Kijima, I. Kawada, H. Tanaka, T. Yamane, J. Am. Ceram. Soc. 58 (1975) 90.
[10] R. Grun, Acta Crystallogr. B 35 (1979) 800.
[11] G. Gundiah, G.V. Madhav, A. Govindaraj, Md.M. Seikh, C.N.R. Rao, J. Mater. Chem. 12 (2002) 1606.
[12] Y.J. Zhang, N.L. Wang, S.P. Gao, R.R. He, S. Miao, J. Liu, J. Zhu, X. Zhang, Chem. Mater. 14 (2002) 3564.
[13] Y.J. Zhang, N.L. Wang, R.R. He, X.Z. Zhang, J. Liu, J. Zhu, J. Cryst. Growth 233 (2001) 803.
[14] H.Y. Kim, J. Park, H. Yang, Chem. Phys. Lett. 372 (2003) 269.
[15] X.C. Wu, W.H. Song, B. Zhao, W.D. Huang, M.H. Pu, Y.P. Sun, J.J. Du, Solid State Commun. 115 (2000) 683.
[16] W.Q. Han, S.S. Fan, Q.Q. Li, B.L. Gu, Appl. Phys. Lett. 71 (1997) 2271.
[17] F. Wang, G.Q. Jin, X.Y. Guo, Mater. Lett. 60 (2006) 330.
[18] F.M. Gao, W.Y. Yang, Y. Fan, L. An, Nanotechnology 19 (2008) 105602.
[19] P. Elmer, Corporation, PH1 5300 Instrument Manual, USA, 1979.
[20] Y.N. Volgin, Y.I. Ukhanov, Opt. Spectrosc. 38 (1975) 412.
[21] D.S. Chuu, C.M. Dai, W.F. Hsieh, C.T. Tsai, J. Appl. Phys. 69 (1991) 8402.
[22] I.H. Cambell, P.M. Fauchet, Solid State Commun. 58 (1986) 739.
[23] J. Robertson, M.J. Powell, Appl. Phys. Lett. 44 (1984) 415.
[24] J. Robertson, Phil. Mag. B 63 (1991) 47.
[25] C.M. Mo, L.D. Zhang, C.Y. Xie, T. Wang, J. Appl. Phys. 73 (1993) 5185.
[26] S.V. Deshpande, E. Gulari, S.W. Brown, S.C. Rand, J. Appl. Phys. 77 (1995) 6534.
[27] Y.Z. Liu, Y.Q. Zhou, W.Q. Shi, L.L. Zhao, B.Y. Sun, T.C. Ye, Mater. Lett. 58 (2004) 2397.
[28] X. Liu, J. Zhu, C.H. Jin, L.M. Peng, D.M. Tang, H.M. Cheng, Nanotechnology 19 (2008) 08571.
[29] J. Luo, Y. Xing, J. Zhu, D. Yu, Y. Zhao, L. Zhang, H. Fang, Z. Huang, J. Xu, Adv. Funct. Mater. 16 (2006) 1081.
[30] Z. Zhang, K. Yao, Y. Liu, C. Jin, X. Liang, Q. Chen, L.M. Peng, Adv. Funct. Mater. 17 (2007) 2478.
[31] M. Ahmad, J. Zhao, C. Pan, J. Zhu, Sci. China Ser. E-Tech. Sci. 52 (2009) 1.